Journal of Power Sources 251 (2014) 152–156

Contents lists available at ScienceDirect

Journal of Power Sources

journal homepage: www.elsevier.com/locate/jpowsour

Short communication

# High efficiency $CH_3NH_3PbI_{(3-x)}Cl_x$ perovskite solar cells with poly(3-hexylthiophene) hole transport layer

Francesco Di Giacomo [a,1], Stefano Razza [a,1], Fabio Matteocci [a], Alessandra D'Epifanio [b], Silvia Licoccia [b], Thomas M. Brown [a], Aldo Di Carlo [a,*]

[a] CHOSE – Center for Hybrid and Organic Solar Energy, Department of Electrical Engineering, University of Rome "Tor Vergata", via del Politecnico 1, 00133 Rome, Italy
[b] Department of Chemical Science and Technologies, University of Rome "Tor Vergata", Via della Ricerca Scientifica 00133 Rome, Italy

## HIGHLIGHTS

- Perovskite solar cells with doped P3HT hole transporter were fabricated.
- For the first time doped P3HT was used with $CH_3NH_3PbI_{(3-x)}Cl_x$ perovskite.
- Best cells showed efficiency up to 9.3%, the record for P3HT solar cells.
- Doped P3HT cells showed a high $V_{OC}$ up to 1.01 V.
- $TiO_2$ dehydration step has been introduced in device fabrication process.

## ARTICLE INFO

*Article history:*
Received 10 September 2013
Received in revised form
8 November 2013
Accepted 15 November 2013
Available online 1 December 2013

*Keywords:*
Perovskite solar cell
Doped P3HT
Thin film photovoltaics
Organometal Halide Perovskite

## ABSTRACT

We fabricate perovskite based solar cells using $CH_3NH_3PbI_{3-x}Cl_x$ with different hole-transporting materials. The most used 2,2′,7,7′-tetrakis-(*N*,*N*-di-p-methoxyphenylamine)9,9′-spirobifluorene (Spiro-OMeTAD) has been compared to the poly(3-hexylthiophene-2,5-diyl) (P3HT). By tuning the energy level of P3HT and optimizing the device's fabrication, we reached 9.3% of power conversion efficiency, which is the highest reported efficiency for a solar cell using P3HT. This result shows that P3HT can be a suitable low cost hole transport material for efficient perovskite based solar cells.



## 1. Introduction

Nowadays, photovoltaic (PV) materials and associated manufacturing processes are under intensive research and development [1] to increase device efficiency, reduce cost and enable new applications for solar energy. In fact, even though silicon solar cells have reached efficiencies of up to 25% for single crystal Si [2] and 20.4% for multi-crystalline Si [3], the production of such material requires energetically demanding processes (such as Si ingot purification) and relatively expensive production lines [4]. On the other hand, thin film technologies have been proved [5] to reduce material costs and energy payback time. Amorphous silicon, CdTe and $Cu(In,Ga)Se_2$ technologies have been extensively investigated [5] and have already found commercial application. More recently, new concepts for delivering solution-processed photovoltaics have been introduced to further simplify the manufacturing process to increase fabrication throughput and reliability and to reduce cost. Among solution based photovoltaics, Dye Solar Cells (DSC) represent a new class of electrochemical solar cells [6] based on sensitized mesoporous $TiO_2$, a liquid electrolyte and a catalyst layer in a sandwich-like architecture. This kind of device allows achievement of efficiencies of up to 12.3% [7] whilst using simple production processes and equipment. However, the liquid electrolyte may still be problematic [8,9] for the production and stability of devices. In this class of cells, solid state DSCs (SDSCs) have been proposed to replace the liquid electrolyte with a hole transport material (HTM). The most commonly used HTM is (2,2′,7,7′-tetrakis-(*N*,*N*-di-p-

* Corresponding author. Tel.: +39 (0)6 72597456.
*E-mail address:* aldo.dicarlo@uniroma2.it (A. Di Carlo).
[1] Both authors contributed equally to this work.

0378-7753/$ – see front matter © 2013 Elsevier B.V. All rights reserved.
http://dx.doi.org/10.1016/j.jpowsour.2013.11.053

methoxyphenylamine)9,9′-spirobifluorene) (Spiro-OMeTAD) [10], which presents efficient charge transport, low recombination rates and also good pore filling of the $TiO_2$ layer enhancing device performance with respect to polymer HTMs. For the sake of lowering costs of the technology, poly(3-hexylthiophene-2,5-diyl) (P3HT) has been employed as a cheaper alternative for small [11] and large area [12] devices. This material shows relatively high hole mobility and can be deposited with several kinds of coating techniques [13,14], such as spin coating, spray coating, slot dye, inkjet printing, and electro-polymerization. Two main issues are commonly linked to P3HT. The size of the polymeric chain reduces the pore filling of the mesoporous $TiO_2$ layer [15], limiting the maximum thickness of $TiO_2$ layer and thus of dye absorption. Furthermore, a tight control of coating parameters and on the additives used is needed to achieve the regular morphology required to improve interchain hopping. By controlling these factors P3HT devices with Power Conversion Efficiency (PCE) of up to 4.5% have been fabricated [16].

Recently, a new class of hybrid organic halide perovskite was introduced as light harvesting material, showing strong absorption in a broad region of the visible spectrum (direct energy gap down to ~1.55 eV [17]), good electron and hole conductivity, delivering also high open circuit voltages in photovoltaic devices. A PCE of 10.2% has been reported [18] using a $CH_3NH_3PbI_{3-x}Cl_x$ sensitized $TiO_2$ together with Spiro-OMeTAD as HTM. By replacing $TiO_2$ with $Al_2O_3$ a PCE of 12.3% was obtained [19]. In the latter case, the electrons are transported directly by the perovskite layer, which is anchored to a mesoporous $Al_2O_3$ scaffold. Remarkably, this kind of perovskite can be processed in air, which makes it a good candidate for industrial use. Another way to improve the performance of $TiO_2$/perovskite solar cells is to modify the $TiO_2$ surface using a self-assembled monolayer of $C_{60}$ fullerenes [18] reaching 11.7% PCE with Spiro-OMeTAD and 6.7% PCE with P3HT, while without $C_{60}$ the efficiency was 10.2% and 3.8%, respectively. Regarding the HTM material coupled with a $CH_3NH_3PbI_3$ perovskite, alternatives to Spiro-OMeTAD have been explored [20] reaching 12% efficiency with poly-triarylamine (PTAA) and 6.7% with P3HT. The high efficiency reached with PTAA already showed how polymer HTMs can lead to similar or even superior performance when systematically compared to Spiro-OMeTAD since pore filling by the HTM is not required anymore in this type of cell where the $TiO_2$ is capped by a layer of perovskite. However, the highest efficiency with perovskite materials was still obtained with Spiro-OMeTAD in the last works which showed efficiency equal or higher than 15% [21,22]. On the other hand, in these works the perovskite synthesis was different to the standard procedures and no comparison with polymeric HTM was performed.

In this paper, we show how P3HT can be a suitable HTM for efficient perovskite based solar cells. We propose an FTO/$TiO_2$/$CH_3NH_3PbI_{3-x}Cl_x$/P3HT/Au architecture (scheme reported in Fig. S1) with the intention of optimizing the performance of P3HT based perovskite solar cell. For the first time doped P3HT is used in combination with $CH_3NH_3PbI_{3-x}Cl_x$, reaching a final device efficiency of 9.3%, which is, to the best of our knowledge, the highest reported efficiency for a solar cell using P3HT as a hole extractor and transporter. In order to assess results, we compare the P3HT cells with similar ones made with Spiro-OMeTAD. The use of P3HT, albeit showing a higher recombination rate respect to Spiro-OMeTAD [23], permits an easy, low cost scaling up of the cell promoting industrial exploitation of this technology.

## 2. Experimental

In order to create the desired electrode pattern, FTO/glass substrates (Pilkington, 8 Ω $\square^{-1}$, 25 mm × 25 mm) were etched via raster scanning laser (Nd:YVO4 pulsed at 30 kHz average output power $P = 10$ W), 4 cells were formed on each substrate. Patterned substrates were cleaned by ultrasonic bath, using detergent, acetone and isopropanol. A compact $TiO_2$ film was deposited onto the FTO surface by Spray Pyrolysis Deposition (SPD) technique using a previously reported procedure [16]. Onto the substrates with the $TiO_2$ compact a thin film of $TiO_2$ nanoparticles based paste (18NR-T Dyesol diluted with terpineol, ethilcellulose, isopropanol and ethanol) was screen-printed and successively sintered at 480 °C for 30 min. The final thickness of the n-$TiO_2$ film was measured via profilometer (Dektak Veeco 150). Profiles were smoothed using Origin 8.5 Software. To dehydrate the samples, these were heated at 120 °C for 60 min in oven. UV irradiation was performed with an estimated power density of 225 mW $cm^{-2}$ (Dymax EC 5000 UV lamp with a metal-halide bulb PN38560 Dymax that contains no UV-C).

Methylammonium iodide was synthesized following a previously reported procedure [24], while $PbCl_2$ (Aldrich, 98%) was used as received. The perovskite was deposited by spin coating (2000 rpm for 60 s) from a dimethylformamide (DMF) solution of methylammonium iodide and $PbCl_2$ (3:1 M ratio) in ambient condition which formed the perovskite after heating to 120 °C for 60 min and a second profile was measured. There was no control over the humidity during the fabrication and characterization processes. The mean humidity was equal to 60% and ambient temperature was 25 °C.

The hole-transporting material (HTM) was deposited in the first case by spin coating a solution of 2,20,7,70-tetrakis-(*N*,*N*-dip-methoxyphenylamine)9,9′-spirobifluorene (Spiro-OMeTAD) at 2000 rpm for 60 s in ambient condition and left in air overnight in a closed box containing silica desiccant. In the second case, the hole-transporting layer was obtained by a spin coating in nitrogen atmosphere (glove box) a P3HT solution in chlorobenzene (Merck 15 mg $mL^{-1}$, MW = 94,100 g $mol^{-1}$), with the following parameters: 600 rpm for 12 s and finally at 2000 rpm for 40 s. $LiN(CF_3SO_2)_2N$ (25 mM, Aldrich) and 4-tert-butylpyridine (TBP, 76 mM) were added to both HTM solutions on the spin coating solution. After HTM deposition a third profile was measured. Samples were introduced into a high vacuum chamber ($10^{-6}$ mbar) in order to evaporate Au back contacts (thickness 100 nm) by thermal evaporation. An evaporation mask defined a device area of 0.1 $cm^2$ (2 × 5 mm).

Masked devices (3 × 6 mm aperture) were tested under a solar simulator (KHS Solar Contest 1200 Class B) at AM1.5 and 100 mW $cm^{-2}$ illumination conditions calibrated with a Skye SKS 1110 sensor, using a Keithley 2420 as a source-metre in ambient condition without sealing. Sun simulator spectrum was measured with a BLACK-Comet UV–VIS Spectrometer (range 190–900 nm). The sun simulator is class B in the visible and near-infrared range (class B between 700 and 800 nm and class A in the rest of the 400–1100 nm range) and has a spatial uniformity less than ±5%. Incident photon-to-current conversion efficiency (IPCE) was measured using an apparatus made of an amperometer (Keithley 2612) and a monochromator (Newport Mod. 74000). UV–vis spectra were measured with a Shimadzu UV-2550 (PC)/MPC 2200 spectrophotometer together with an integrating sphere. X-ray diffraction (XRD) analysis was performed to investigate the phases of the samples, using a Philips X-Pert Pro 500 diffractomer with Cu Ka radiation.

## 3. Results and discussion

The compact $TiO_2$ (c-$TiO_2$) synthesis process and thickness were previously optimized [16] on an SDSC for efficient charge collection and for avoiding recombination of electrons from the FTO back into the active layer. Adding acetylacetone (ACAC) to a conventional

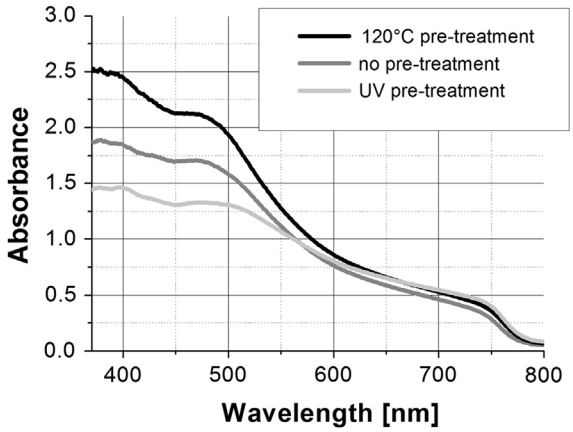


**Fig. 1.** Absorbance spectra of $TiO_2/CH_3NH_3PbI_{(3-x)}Cl_x$ on FTO glass. The black line is relative to a dehydrated $TiO_2$ sample, the light grey to a UV-treated sample, and the dark grey to a sample without any treatment. $TiO_2$ thickness was equal to 700 nm and a 40% w/w perovskite precursor solution was spin coated at 2000 RPM and annealed at 120 °C for 1 h. All measurements were carried out using an integrating sphere. Absorbance of FTO/glass was subtracted for all samples.

precursor solution for spray pyrolysis deposition of c-$TiO_2$ layers has been shown to enhance the blocking effect and consequently of the diode-like behaviour of the cell. This is crucial to avoid any current loss at the FTO interface. ACAC enhances the adhesion of c-$TiO_2$ over the FTO reducing the charge transfer resistance at their interface. The compact layer thickness we used is larger than most found in the literature for perovskite solar cell (120 nm respect to 50–60 nm [19,20]). P3HT was blended with $LiN(CF_3SO_2)_2N$ (Lithium TFSI) salt and tert-butylpiridine. These additives are used in SDSCs to improve device efficiency by doping the HTM, and have also been used on perovskite solar cells [20,23]. Further optimizations were performed on the $TiO_2$ paste formulation and a pre-treatment was introduced on the sintered porous $TiO_2$. To obtain a thickness of 700 nm by screen printing we diluted the commercial 18 NR-T Dyesol paste. If the dilution was performed only with ethanol a very rough surface was obtained, so the 18 NR-T paste was blended with a mixture of terpineol, ethylcellulose, isopropanol and ethanol in order to preserve the thixotropic behaviour and to allow the formation of a flat $TiO_2$ layer. Since it is well known that this class of perovskites is very unstable in the presence of moisture [25],due to the presence of the hygroscopic amine salt, a further improvement was obtained by dehydration of the $TiO_2$ prior to spin coating the perovskite solution. Dehydration was performed by heating the sintered $TiO_2$ at 120 °C for at least 1 h. To maintain dehydration, the samples were kept in a dry environment while cooling to room temperature. To further clean the $TiO_2$ surface [26], some samples were UV irradiated with 200 mW $cm^{-2}$ incident power using an Hg lamp. The perovskite absorbance spectra are shown in Fig. 1 for all the different samples. An increase in the absorbance can be noticed for the dehydrated samples, while the UV-treated samples showed smaller absorbance. The reason for the lower absorbance can be ascribed to the hydrophilic behaviour of the $TiO_2$ induced by the UV treatment [27], which increases the absorption of water on the titania surface. The perovskite layer was further characterized with X-ray diffraction analysis shown in Fig. S2, All characteristic diffraction peaks of the perovskite structure were observed at angles of 14.17°, 28.38° 40.5° and 43.1° which suggest that the films fabricated on glass substrates were single phase. By adopting all the previous optimization steps, a batch of 66 devices using P3HT and Spiro-OMeTAD was realized and the PCE and open circuit voltage ($V_{OC}$) are shown in Fig. 2, while fill factor (FF) and short circuit current ($J_{SC}$) are shown in Fig. S3. The PCE and open circuit voltage ($V_{OC}$) histograms allowed us to statistically characterize the P3HT devices also in comparison with the Spiro based cells. For each histogram a Gaussian fit of the distribution was also plotted. The average efficiency of P3HT devices was $(6.6 \pm 1.7)$% while the most efficient cell had a PCE of 9.3%. These values are very close to the Spiro-OMeTAD based cells, which reach an average PCE of $(5.9 \pm 1.3)$%. We obtained several devices with efficiency over the

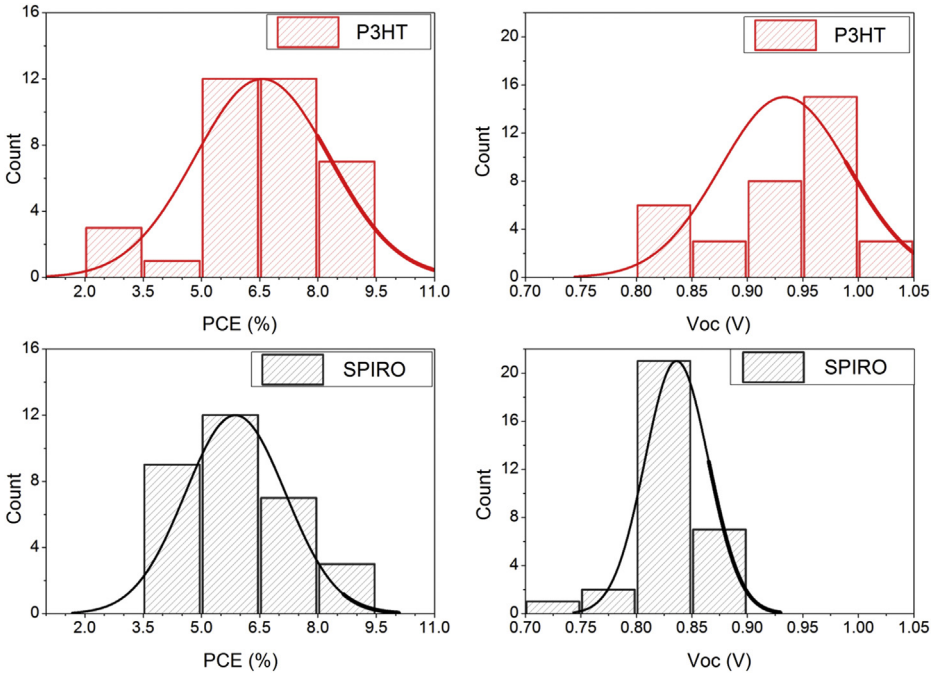


**Fig. 2.** Histograms of the PCE (left side) and $V_{OC}$ (right side) for a single batch of 66 solar cells with an FTO/c-$TiO_2$/nc-$TiO_2$/$CH_3NH_3PbI_{(3-x)}Cl_x$/HTM/Au architecture, with P3HT (red bar upper side) and Spiro (black bar lower side) as HTM. (For interpretation of the references to colour in this figure legend, the reader is referred to the web version of this article.)

previously reported record [20] for P3HT based device. Regarding the other PV parameters, both kind of devices showed similar FF, 60 ± 5% for Spiro and 58 ± 5% for P3HT, and $J_{SC}$, 12 ± 2 mA cm$^{-2}$ for Spiro and 12 ± 3 mA cm$^{-2}$ for P3HT, while there is a clear enhancement of $V_{OC}$ in the P3HT devices. In fact, the $V_{OC}$ of P3HT devices is 0.93 ± 0.06 V which is higher than 0.84 ± 0.03 V obtained with Spiro-OMeTAD (an 8% average increase). This phenomenon can be ascribed to the different ionization potentials (HOMO) of the HTMs (5.0–5.1 eV for Spiro [28] and 5.1–5.2 eV for P3HT [29]) together with a photoinduced oxidative p-doping of the P3HT [30,31], which can further increase the ionization potential. Even in this latter case, hole injection from the perovskite to the HTM is possible since the valence band of $CH_3NH_3PbI_{3-x}Cl_x$ lies at 5.3 eV [32].

In Fig. 3 the *JV* curves for the best P3HT and Spiro-OMeTAD based cells (9.3% and 8.6% PCE, respectively) are reported. The two curves are very similar in all characteristics besides the $V_{OC}$. To further characterize the two devices, the series resistance and the shunt resistance were measured by evaluating the slope of the *JV* curves at open circuit and short circuit conditions, respectively. The results showed that while the series resistances of the devices are equal (8 Ω cm$^2$ for both), the shunt resistances are slightly different (295 Ω cm$^2$ for P3HT and 365 Ω cm$^2$ for Spiro-OMeTAD), due to the higher recombination rate of P3HT [23] as HTM. However, the significant increase of the $V_{OC}$ discussed earlier results in a more efficient P3HT device.

To further characterize the cells' architecture, the thickness of the multilayer was recorded after each deposition step (sintered mesoporous $TiO_2$ over the c-$TiO_2$, annealed perovskite, and dried P3HT) starting from the edge of the sample (clean FTO area) towards the centre of the cell. Each thickness profile was taken along the same line to study the deposition of each layer on the previous one. Results shown in Fig. 4 can be gauged considering the device architecture reported in Fig. S1. The first step present between 2700 and 3500 μm is relative to the 120 nm thick $TiO_2$ compact layer. The mesoporous $TiO_2$ layer overlaying the compact layer is 700 nm thick. The thickness profile of the perovskite layer shows a high roughness over the $TiO_2$ layer, meaning that the part of the perovskite material raises above the mesoporous structure. Since the thickness profile after the subsequent P3HT deposition shows a much flatter surface, it is possible that the roughness of the perovskite had arisen from the profilometer's tip collecting material during profiling, or from weakly bonded perovskite crystals

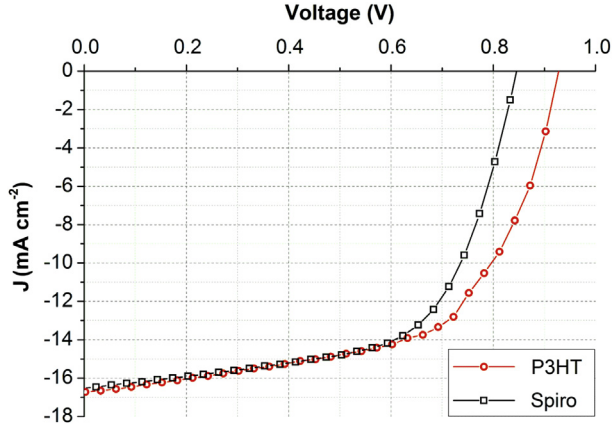


**Fig. 3.** Current density–voltage (*JV*) curves of the best FTO/c-$TiO_2$/nc-$TiO_2$/$CH_3NH_3PbI_{(3-x)}Cl_x$/P3HT/Au (red line and symbols) and FTO/c-$TiO_2$/nc-$TiO_2$/$CH_3NH_3PbI_{(3-x)}Cl_x$/Spiro-OMeTAD/Au (black line and symbol) solar cells. (For interpretation of the references to colour in this figure legend, the reader is referred to the web version of this article.)

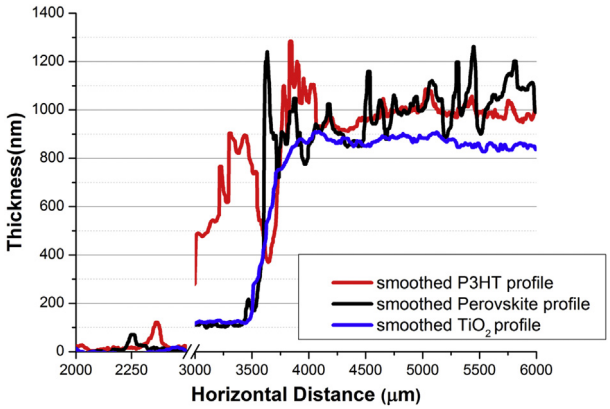


**Fig. 4.** Thickness profiles taken after $TiO_2$ sintering (blue line), after perovskite annealing (black line) and after P3HT drying (red line) over a c-$TiO_2$/FTO/glass substrate. All measurements were taken on the same area of the same device, and the raw data were smoothed to remove noise. (For interpretation of the references to colour in this figure legend, the reader is referred to the web version of this article.)

which were then removed by spin coating the P3HT overlayer. The presence of this perovskite capping layer (already reported in literature [19,20]) led to efficient P3HT based devices compared to a solid state DSC, since there is no strict requirement of pore filling into the $TiO_2$ structure. Indeed the PCE of the P3HT based devices is very similar if not greater than the equivalent Spiro-OMeTAD based cells. On the other hand, if the same comparison is made with SDSCs, a 47% PCE lowering using P3HT instead of Spiro-OMeTAD was reported [33]. These results show that P3HT, as well as PTAA, can be a suitable HTM for efficient and low cost perovskite based solar cells, thanks to an appropriate HOMO level and because pore filling is not a requirement for this type of cells.

## 4. Conclusion

We showed how doped P3HT can be a suitable HTM for efficient perovskite based solar cells, fabricating devices with PCE up to 9.3% and high $V_{OC}$. This PCE is, to the best of our knowledge, the highest reported efficiency for a solar cell using P3HT as a hole extractor and transporter. Further efficiency enhancements may be achieved by replacing $TiO_2$ with $Al_2O_3$, which has been shown [24] to improve the overall performance of cells. Other improvements can be sought by tailoring the perovskite composition (e.g. Br addition [25]) or by using the recently developed two-step synthesis [21].

## Acknowledgements

Thanks are due to Ms C. D'Ottavi for her valuable technical support. The authors thank Dr Girolamo Micuzzi for laser etching, Martina Dianetti for Au evaporation and Andrea Zampetti for useful discussion. We acknowledge "Polo Solare Organico" Regione Lazio and the "DSSCX" MIUR-PRIN2010 for funds. F. Di Giacomo and S. Razza contributed equally to this work.

## Appendix A. Supplementary data

Supplementary data related to this article can be found at http://dx.doi.org/10.1016/j.jpowsour.2013.11.053.

## References

[1] N.G. Dhere, R.G. Dhere, J. Vacuum Sci. Technol. A 23 (2005) 1208–1214.
[2] J. Zhao, A. Wang, M.A. Green, Solar Energy Mater. Sol. Cells 66 (2001) 27–36.
[3] O. Schultz, S.W. Glunz, G.P. Willeke, Prog. Photovoltaics Res. Appl. 12 (2004) 553–558.

[4] G. Solar, 2013 http://www.3gsolar.com/why-3g.
[5] S. Hegedus, Prog. Photovoltaics Res. Appl. 14 (2006) 393–411.
[6] B. O'Regan, M. Grätzel, Nature 353 (1991) 737–740.
[7] A. Yella, H.-W. Lee, H.N. Tsao, C. Yi, A.K. Chandiran, M.K. Nazeeruddin, E.W.-G. Diau, C.-Y. Yeh, S.M. Zakeeruddin, M. Grätzel, Science 334 (2011) 629–634.
[8] M.I. Asghar, K. Miettunen, J. Halme, P. Vahermaa, M. Toivola, K. Aitola, P. Lund, Energy Environ. Sci. 3 (2010) 418–426.
[9] S. Mastroianni, A. Lanuti, S. Penna, A. Reale, T.M. Brown, A. Di Carlo, F. Decker, Chemphyschem 13 (2012) 2925–2936.
[10] I.K. Ding, N. Tétreault, J. Brillet, B.E. Hardin, E.H. Smith, S.J. Rosenthal, F. Sauvage, M. Grätzel, M.D. McGehee, Adv. Funct. Mater. 19 (2009) 2431–2436.
[11] W. Zhang, R. Zhu, F. Li, Q. Wang, B. Liu, J. Phys. Chem. C 115 (2011) 7038–7043.
[12] F. Matteocci, S. Casaluci, S. Razza, A. Guidobaldi, T.M. Brown, A. Reale, A. Di Carlo, J. Power Sources 246 (2014) 361–364.
[13] R. Søndergaard, M. Hösel, D. Angmo, T.T. Larsen-Olsen, F.C. Krebs, Mater. Today 15 (2012) 36–49.
[14] E.L. Ratcliff, J.L. Jenkins, K. Nebesny, N.R. Armstrong, Chem. Mater. 20 (2008) 5796–5806.
[15] J. Melas-Kyriazi, I.K. Ding, A. Marchioro, A. Punzi, B.E. Hardin, G.F. Burkhard, N. Tétreault, M. Grätzel, J.-E. Moser, M.D. McGehee, Adv. Energy Mater. 1 (2011) 407–414.
[16] F. Matteocci, G. Mincuzzi, F. Giordano, A. Capasso, E. Artuso, C. Barolo, G. Viscardi, T.M. Brown, A. Reale, A. Di Carlo, Org. Electron. 14 (2013) 1882–1890.
[17] E. Mosconi, A. Amat, M.K. Nazeeruddin, M. Grätzel, F. De Angelis, J. Phys. Chem. C 117 (2013) 13902–13913.
[18] A. Abrusci, S.D. Stranks, P. Docampo, H.-L. Yip, A.K.Y. Jen, H.J. Snaith, Nano Lett. 13 (2013) 3124–3128.
[19] J.M. Ball, M.M. Lee, A. Hey, H.J. Snaith, Energy Environ. Sci. 6 (2013) 1739–1743.
[20] J.H. Heo, S.H. Im, J.H. Noh, T.N. Mandal, C.S. Lim, J.A. Chang, Y.H. Lee, H.J. Kim, A. Sarkar, M.K. Nazeeruddin, M. Grätzel, S.I. Seok, Nat. Photonics 7 (2013) 486–491.
[21] J. Burschka, N. Pellet, S.-J. Moon, R. Humphry-Baker, P. Gao, M.K. Nazeeruddin, M. Grätzel, Nature 499 (2013) 316–319.
[22] M. Liu, M.B. Johnston, H.J. Snaith, Nature 501 (2013) 395–398.
[23] D. Bi, L. Yang, G. Boschloo, A. Hagfeldt, E.M.J. Johansson, J. Phys. Chem. Lett. 4 (2013) 1532–1536.
[24] M.M. Lee, J. Teuscher, T. Miyasaka, T.N. Murakami, H.J. Snaith, Science 338 (2012) 643–647.
[25] J.H. Noh, S.H. Im, J.H. Heo, T.N. Mandal, S.I. Seok, Nano Lett. 13 (2013) 1764–1769.
[26] V. Zardetto, F. Di Giacomo, D. Garcia-Alonso, W. Keuning, M. Creatore, C. Mazzuca, A. Reale, A. Di Carlo, T.M. Brown, Adv. Energy Mater. 3 (2013) 1292–1298.
[27] T. Zubkov, D. Stahl, T.L. Thompson, D. Panayotov, O. Diwald, J.T. Yates, J. Phys. Chem. B 109 (2005) 15454–15462.
[28] T. Leijtens, I.K. Ding, T. Giovenzana, J.T. Bloking, M.D. McGehee, A. Sellinger, ACS Nano 6 (2012) 1455–1462.
[29] H. Chen, X. Pan, W. Liu, M. Cai, D. Kou, Z. Huo, X. Fang, S. Dai, Chem. Commun. 49 (2013) 7277–7279.
[30] H.-H. Liao, C.-M. Yang, C.-C. Liu, H. Sheng-Fu, M. Hsin-Fei, S. Jow-Tsong, J. Appl. Phys. 103 (2008) 104506–104508.
[31] C.-K. Lu, H.-F. Meng, Phys. Rev. B 75 (2007) 235206.
[32] A. Abrusci, S.D. Stranks, P. Docampo, H.-L. Yip, A.K.Y. Jen, H.J. Snaith, Nano Lett. (2013).
[33] L. Yang, U.B. Cappel, E.L. Unger, M. Karlsson, K.M. Karlsson, E. Gabrielsson, L. Sun, G. Boschloo, A. Hagfeldt, E.M.J. Johansson, Phys. Chem. Chem. Phys. 14 (2012) 779–789.